

Liquefaction at Strong Motion Stations and in Urayasu City during the 2011 Tohoku-Oki Earthquake

Brady R. Cox,^{a)} M.EERI, Ross W. Boulanger,^{b)} M.EERI, Kohji Tokimatsu,^{c)} M.EERI, Clinton M. Wood,^{a)} Akio Abe,^{d)} Scott Ashford,^{e)} Jennifer Donahue,^{f)} Kenji Ishihara,^{g)} Robert Kayen,^{h)} Kota Katsumata,^{c)} Tadahiro Kishida,ⁱ⁾ Takaji Kokusho,^{g)} H. Benjamin Mason,^{e)} M.EERI, Robb Moss,^{j)} Jonathan P. Stewart,^{k)} M.EERI, Kazushi Tohyama,^{c)} and Dimitrios Zekkos^{l)}

The 2011 $M_w = 9.0$ Tohoku-oki earthquake generated a large number of unique soil liquefaction case histories, including cases with strong ground motion recordings on liquefiable or potentially liquefiable soils. We have compiled a list of 22 strong motion stations (SMS) where surface evidence of liquefaction was observed and 16 SMS underlain by geologically recent sediments or fills where surface evidence of liquefaction was not observed. Pre-earthquake standard penetration test data and borehole shear wave velocity (V_s) profiles are available for some stations, but critical information, such as grain size distribution and fines plasticity, are often lacking. In the heavily damaged city of Urayasu, we performed post-earthquake cone penetration testing at seven SMS and V_s profiles, using surface wave methods at 28 additional locations to supplement existing geotechnical data. We describe the liquefaction effects in Urayasu, the available site characterization data, and our initial data interpretations. [DOI: 10.1193/1.4000110]

INTRODUCTION

Case histories of soil liquefaction in the 11 March 2011 $M_w = 9.0$ Tohoku-oki (or Great East Japan) earthquake provide important opportunities for learning about the seismic performance of a wide range of geotechnical systems and constructed facilities. High-quality liquefaction case histories for large-magnitude events are rare and have the potential to yield insights on the triggering of liquefaction and subsequent performance of facilities, under long

^{a)} University of Texas, Department of Civil, Architectural and Environmental Engineering, Austin, TX 78730

^{b)} University of California at Davis, Department of Civil and Environmental Engineering, Davis, CA 95616

^{c)} Tokyo Institute of Technology, Dept. of Architecture and Building Engineering, Tokyo, 152-8552 Japan

^{d)} Tokyo Soil Research Co., Ltd., Tokyo, 152-0021 Japan

^{e)} Oregon State University, School of Civil and Construction Engineering, Corvallis, OR 97331

^{f)} Geosyntec, 1111 Broadway, Oakland, CA 94607

^{g)} Chuo University, Tokyo, 136-8577 Japan

^{h)} U.S. Geological Survey, Menlo Park, CA 94025

ⁱ⁾ Pacific Earthquake Engineering Research Center, University of California, Berkeley, CA 94720

^{j)} Cal Poly State University, Department of Civil and Environmental Engineering, San Luis Obispo, CA 93407

^{k)} University of California, Los Angeles, Dept. of Civil and Env. Engineering, Los Angeles, CA 90095

^{l)} University of Michigan, Department of Civil and Environmental Engineering, Ann Arbor, MI 48109

durations of shaking. The opportunities for learning from this event are particularly unique because of the extensive network of strong ground motion recording stations in Japan and the significant amount of detailed geotechnical data and performance observations being compiled. This information has been gathered through a number of organizations and individuals involved in post-earthquake reconnaissance efforts and subsequent research studies. In particular, teams from the Geotechnical Extreme Events Reconnaissance (GEER) Association participated in geotechnical reconnaissance efforts with the support and collaboration of numerous colleagues in Japan. A total of 25 GEER members worked with more than 26 Japanese counterparts in investigations of site response, liquefaction, levees, dams, ports, bridges, and lifelines. The resulting data and observations have been compiled by GEER members (e.g., Boulanger 2012, Kayen et al. 2012b, GEER 2011a, 2011b, 2011c, 2011d; <http://geerassociation.org/>) and Japanese colleagues (e.g., Tokimatsu et al. 2012, Tokimatsu and Katsumata 2012, Katsumata and Tokimatsu 2012, Ishihara et al. 2011, Tokimatsu et al. 2011, Tsukamoto et al. 2012).

This paper primarily focuses on liquefaction, or the lack thereof, at strong motion stations (SMS) in the affected regions and across the well-instrumented and heavily damaged city of Urayasu. Stewart et al. (2013, this issue) describe the general strong motion attributes of this earthquake and the inventory of ground motion data. We focus on a relatively small subset of recordings that are relevant from a liquefaction perspective. This subset includes 22 SMS where liquefaction was evidenced by observations of surface ejecta and/or visible ground deformations (i.e., settlement, cracking, or spreading) following the earthquake (Table 1) and 16 SMS underlain by geologically recent sediments or fills where surface evidence of liquefaction or ground failure (deformations) was not observed (Table 2). Most of the investigated SMS are located at the southern end of the fault rupture in the Kanto Plain and Tokyo Bay regions (Figure 1). It is possible that liquefaction occurred at other stations along the coastline in the affected regions, but the surface evidence may have been obscured by the tsunami. The available ground motion recordings represent a unique set of data that captures the dynamic response and liquefaction of soils during long duration shaking produced by this $M_w = 9.0$ earthquake. As such, these SMS data can be used to anchor liquefaction triggering curves and refine magnitude scaling factors, assess procedures for estimating ground surface deformations, evaluate dynamic site response analysis models for liquefiable soils, and develop insights into soil-structure interaction effects on liquefaction triggering and deformations.

Examinations of the available SMS site characterization data indicate, however, that additional subsurface data are required before liquefaction analyses can be performed confidently for most sites. Prior to the earthquake, Standard Penetration Test (SPT) and down-hole shear wave velocity (V_s) profiles were available for only some of the SMS of interest, as summarized in Tables 1 and 2. For example, we have been able to locate SPT data at only three of the 22 SMS where evidence of liquefaction was observed and at nine of the 16 SMS on geologically recent sediments or fills where evidence of liquefaction was not observed. Furthermore, critical information, such as grain size distribution and fines plasticity, are generally lacking at all sites, which introduces significant uncertainties in the back-analyses of these case histories. Simplified liquefaction triggering analyses are presented in this paper for select SMS using the available SPT data as a means to illustrate the need to collect additional soil information for quality case history development.

Table 1. List of strong ground motion recording stations with evidence of liquefaction during the M9.0 Tohoku-oki earthquake

Station	Network	Location	Latitude	Longitude	PGA (g)	Liquefaction Severity	Site Characterization Data Source			
							SPT	Borehole V _s	Surf. Wave V _s	SCPT
IBRH20	KIKNET	Kamisu, Ibaraki	35.82860 ³	140.73226 ³	0.220	Moderate; sand boils in vicinity on three sides but not directly around station	-	KIKNET	GEER	-
IBR014	KNET	Tsuchiura, Ibaraki	36.07283 ¹	140.19481 ¹	0.506	Minor; minor sand boils in vicinity	KNET	KNET	GEER	-
CHB014	KIKNET	Choshi, Chiba	35.73425 ³	140.82316 ³	0.173	Minor; small sand boils in vicinity but not directly around station	-	KIKNET	GEER	-
CHB024	KNET	Mihama, Chiba	35.63370 ³	140.07819 ³	0.237	Severe; large sand boils in vicinity and around station	KNET	KNET	GEER	-
Mihama	Chiba University	Mihama, Chiba	35.64888 ¹	140.03411 ¹	0.279	Moderate; liquefaction distress in parking lot, but not immediately around station or building	-	-	-	-
TKY017	KNET	Koto, Tokyo	35.64727 ³	139.80919 ³	0.223	Moderate; sand boils in vicinity on several sides of the station	-	-	GEER	-
Cloverleaf	NILIM	Urayasu, Chiba	35.65488 ³	139.91064 ³	NA	Moderate; sand boils surrounding station and liquefaction around cloverleaf interchange and bridge	-	-	GEER	-
AKE	Keiyo Gas	Urayasu, Chiba	35.64186 ⁴	139.92070 ⁴	0.272	Minor	-	-	-	-
CHI	Keiyo Gas	Urayasu, Chiba	35.62589 ⁴	139.89809 ⁴	0.157	Minor-Moderate	-	-	-	-
CHK	Keiyo Gas	Urayasu, Chiba	35.61958 ⁴	139.89704 ⁴	0.152	Minor-Moderate	-	-	-	-
HIG	Keiyo Gas	Urayasu, Chiba	35.64605 ⁴	139.89362 ⁴	0.238	Minor	-	-	-	-
IMA	Keiyo Gas	Urayasu, Chiba	35.64071 ⁴	139.90213 ⁴	0.171	Moderate	-	-	-	-

(continued)

Table 1. (continued)

Station	Network	Location	Latitude	Longitude	PGA (g) ⁵	Liquefaction Severity	Site Characterization Data Source			
							SPT	Borehole V _s	Surf. Wave V _s	SCPT
IR1	Keiyo Gas	Urayasu, Chiba	35.64802 ⁴	139.91257 ⁴	0.176	Minor	-	-	-	-
IRF	Keiyo Gas	Urayasu, Chiba	35.64889 ⁴	139.91604 ⁴	0.256	Moderate	-	-	-	GEER
JAL	Keiyo Gas	Urayasu, Chiba	35.64597 ⁴	139.92565 ⁴	0.199	Severe	-	-	-	GEER
MHM	Keiyo Gas	Urayasu, Chiba	35.65331 ⁴	139.91070 ⁴	0.176	Moderate	-	-	-	-
MIH	Keiyo Gas	Urayasu, Chiba	35.63458 ⁴	139.88812 ⁴	0.165	Minor-Moderate	-	-	-	-
TKK	Keiyo Gas	Urayasu, Chiba	35.63775 ⁴	139.91561 ⁴	0.213	Moderate	-	-	-	GEER
TKM	Keiyo Gas	Urayasu, Chiba	35.63195 ⁴	139.91901 ⁴	0.222	Severe	-	-	-	GEER
TKS	Keiyo Gas	Urayasu, Chiba	35.63314 ⁴	139.91182 ⁴	0.162	Severe	-	-	-	-
MYG013	KNET	Miyagino, Miyagi	38.26597 ³	140.92858 ³	1.547	Moderate; “Sand boiling occurred in the neighborhood” Tokimatsu & Tamura et al. (2012); ejecta all around station in GEER pics	KNET	KNET	GEER	-
Prefecture	JMA	Kamisu,	35.89035 ¹	140.66437 ¹	0.226	Moderate; liquefaction ejecta on station housing and in vicinity;	-	-	GEER	-
Kamisu		Ibaraki								
City										

Notes:
¹Coordinates Obtained from GEER Records
²Coordinates Obtained from KNET
³Coordinates Obtained Manually via Google Earth
⁴Coordinates Obtained from Keiyo Gas Network
⁵Maximum Horizontal Component

Table 2. List of strong ground motion recording stations on geologically recent sediments or fills without evidence of ground failure during the M9.0 Tohoku-oki earthquake

Station	Network	Location	Latitude	Longitude	PGA (g)	Liquefaction Severity	Site Characterization Data Source			
							SPT	Borehole V _s	Surf. Wave V _s	SCPT
CHB005	KNET	Choshi, Chiba	35.73580 ²	140.83000 ²	0.179	No ground failure; close to CHB014, which had minor liquefaction	KNET	KNET	-	-
CHB008	KNET	Urayasu, Chiba	35.65564 ¹	139.90273 ¹	0.160	No ground failure	KNET	KNET	-	-
AKM	Keiyo Gas	Urayasu, Chiba	35.63770 ⁴	139.92451 ⁴	0.169	No ground failure	-	-	-	GEER
HND	Keiyo Gas	Urayasu, Chiba	35.64219 ⁴	139.93067 ⁴	0.174	No ground failure	-	-	-	GEER
HOS	Keiyo Gas	Urayasu, Chiba	35.66255 ⁴	139.90235 ⁴	0.180	No ground failure	-	-	-	GEER
CHB009	KNET	Chiba, Chiba	35.60759 ¹	140.10774 ¹	0.183	No ground failure	KNET	KNET	-	-
CHB004	KNET	Kashima, Ibaraki	35.90100 ¹	140.49000 ¹	0.307	No ground failure	KNET	KNET	-	-
Chiba-G, GB	PARI	Chuocho, Chiba	35.60171 ¹	140.10272 ¹	0.130	No ground failure	PARI	PARI	GEER	-
IBR016	KNET	Toride, Ibaraki	35.91135 ³	140.04936 ³	0.527	No ground failure	KNET	KNET	GEER	-
Shinagawa-U, UB	PARI	Shinagawa, Tokyo	35.62582 ¹	139.75784 ¹	0.210	No ground failure	PARI	PARI	-	-
Oi-U, UB	PARI	Shinagawa, Tokyo	35.60200 ¹	139.76400 ¹	0.120	No ground failure	PARI	PARI	-	-

(continued)

Table 2. (continued)

Station	Network	Location	Latitude	Longitude	PGA (g) ⁵	Liquefaction Severity	Site Characterization Data Source			
							SPT	Borehole V _s	Surf. Wave V _s	SCPT
TKY013	KNET	Koto, Tokyo	35.66263 ³	139.83413 ³	0.144	No ground failure; instrument tilted about 1.3 degrees	-	-	-	-
TKY016	KNET	Koto, Tokyo	35.64828 ¹	139.79887 ¹	0.164	No ground failure	-	-	-	-
TKY018	KNET	Koto, Tokyo	35.65512 ³	139.81145 ³	0.255	No ground failure; instrument tilted about 1.3 degrees on apparently week fill	-	-	-	-
TKY020	KNET	Koto, Tokyo	35.66452 ¹	139.80863 ¹	0.147	No ground failure	-	-	-	-
KNG002	KNET	Yokohama, Kanagawa	35.43732 ³	139.63309 ³	0.168	No ground failure	KNET	KNET	-	-

Notes:
¹Coordinates Obtained from GEER Records
²Coordinates Obtained from KNET
³Coordinates Obtained Manually via Google Earth
⁴Coordinates Obtained from Keiyo Gas Network
⁵Maximum Horizontal Component

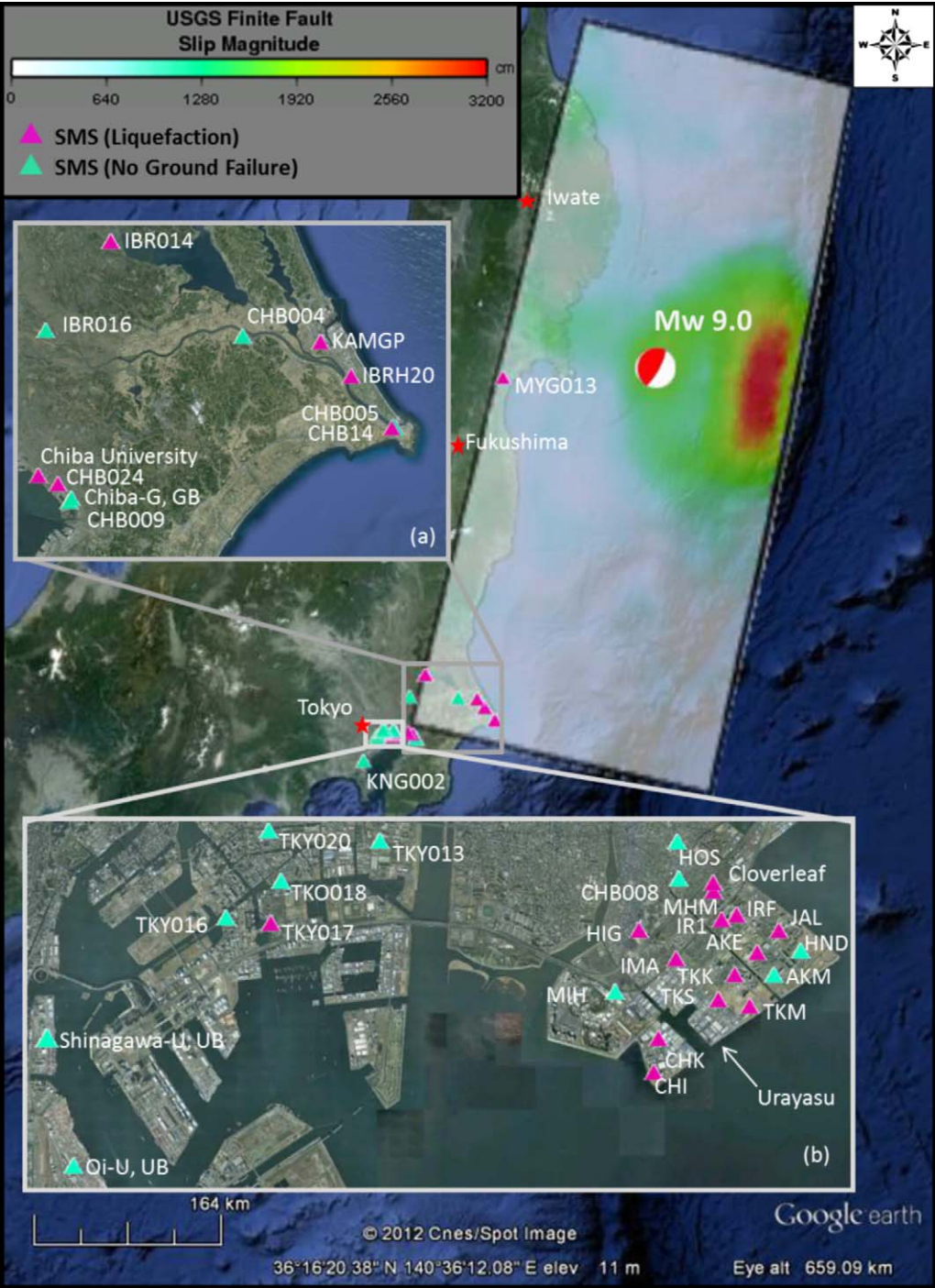


Figure 1. Locations of strong ground motion recording stations with either evidence of liquefaction or underlain by geologically recent sediments or fills with no surface evidence of liquefaction or ground failure.

Liquefaction effects across the heavily damaged city of Urayasu are of particular interest because there are 17 SMS located throughout the city (refer to Figure 1b), and there has been intense liquefaction severity mapping and site characterization efforts by Japanese and GEER researchers following the earthquake. We performed cone penetration testing (CPT) at seven SMS sites in Urayasu City (four with evidence of soil liquefaction and three with no surface evidence of ground failure) as a starting point for detailed characterization at these sites. We also performed V_s profiling using surface wave methods at 28 additional locations throughout Urayasu as a means of investigating potential aging effects in reclaimed fills and examining the ability of V_s data to track the observed spatial variation in liquefaction severity across the city. We describe the observed effects of liquefaction, the new CPT and V_s site characterization data, and our initial interpretations.

LIQUEFACTION AND STRONG MOTION STATIONS

A significant number of strong ground motion recordings were obtained at SMS sites that were underlain by soils that either liquefied during the earthquake or were located on geologically recent sediments or fills where liquefaction might be anticipated, but no ground failure was observed. The occurrence or nonoccurrence of liquefaction was evaluated based on field reconnaissance by the authors, generally performed within two to three weeks of the main shock. A summary of 22 SMS with observed effects of soil liquefaction is provided in Table 1, while summary information for 16 SMS without surface evidence of liquefaction is provided in Table 2. Available information includes the station name, station network, general location, geodetic coordinates, peak horizontal ground acceleration (PGA) values, notes about the severity of liquefaction, and availability of subsurface information, such as SPT, CPT, and V_s data. There currently are some discrepancies in latitude and longitude coordinates for a few of the SMS, and thus footnotes indicate whether the coordinates are from KNET, KIKNET, GEER track logs, or Google Earth imagery. Acceleration time series records are not currently available for all SMS (particularly private network stations). However, PGA values (maximum horizontal component) are provided for all but one station.

The locations of the investigated SMS are shown in Figure 1. The 22 SMS with evidence of liquefaction were mostly located at the southern end of the fault rupture plane in the Tokyo Bay and Kanto Plain regions. Liquefaction evidence was only conclusively documented by our teams at one station near the epicentral region (MYG013; refer to Figure 1). It is possible that liquefaction occurred at other stations along the coastline in the affected regions, but the evidence may have been obscured by the tsunami. In some cases, the recorded ground motions at liquefaction sites show clear evidence of liquefaction, but in other cases, the characteristics of the motions do not clearly exhibit any signs of significant softening or cyclic mobility during strong shaking. An examination of two cases, one with surface evidence of soil liquefaction and one without, is presented to illustrate the differences in behaviors.

KNET station CHB009 (Figure 1a and Table 2) is an example of a station where no surface evidence of liquefaction was noted despite the presence of saturated sands in the subsurface and a PGA value of 0.183 g. The ground surface around the recording station showed no signs of deformation or soil ejecta in the vicinity, as illustrated by the post-earthquake photograph in Figure 2a. The acceleration time series recorded at the station (NIED 2011), as shown in Figure 3, exhibit no evident change in site response characteristics



Figure 2. Two recording stations in Chiba: (a) station CH009 without ground failure, and (b) station CHB024 with extensive sand boils and moderate ground deformations.

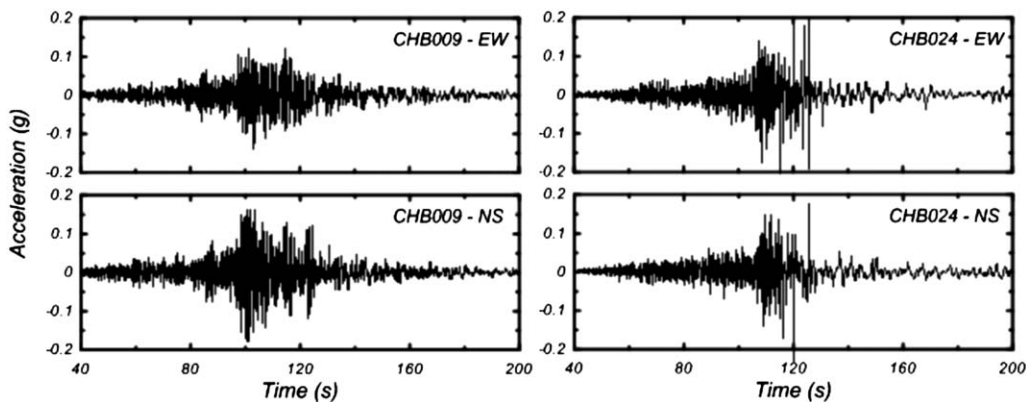


Figure 3. Horizontal ground surface accelerations recorded at CHB009 and CHB024 in Chiba (data from KNET, [NIED 2011](#)).

(e.g., deamplification or period elongation) during shaking, which might be indicative of liquefaction triggering. The soil profile consists of about 3.0 m of fill, overlying about 7.0 m of “sandy soil,” overlying a thick stratum of silt (Figure 4). The water table is estimated to be at a depth of about 3 m. The SPT blow counts, which are assumed to correspond to a typical energy ratio of 75%, are plotted in Figure 4a as N_{60} values. The corresponding cyclic resistance ratios (CRR) for the sandy soil and the earthquake-induced cyclic stress ratios (CSR) computed using the procedures from [Idriss and Boulanger \(2008\)](#) are also shown in Figure 4a. The fines content of the sandy soil is not available, so it was assumed to be 25% based on its visual description. The plasticity of the silt strata is not available, so two scenarios were considered: (1) the silt is nonplastic such that it should be analyzed using liquefaction correlations, or (2) the silt is sufficiently plastic that it should instead be

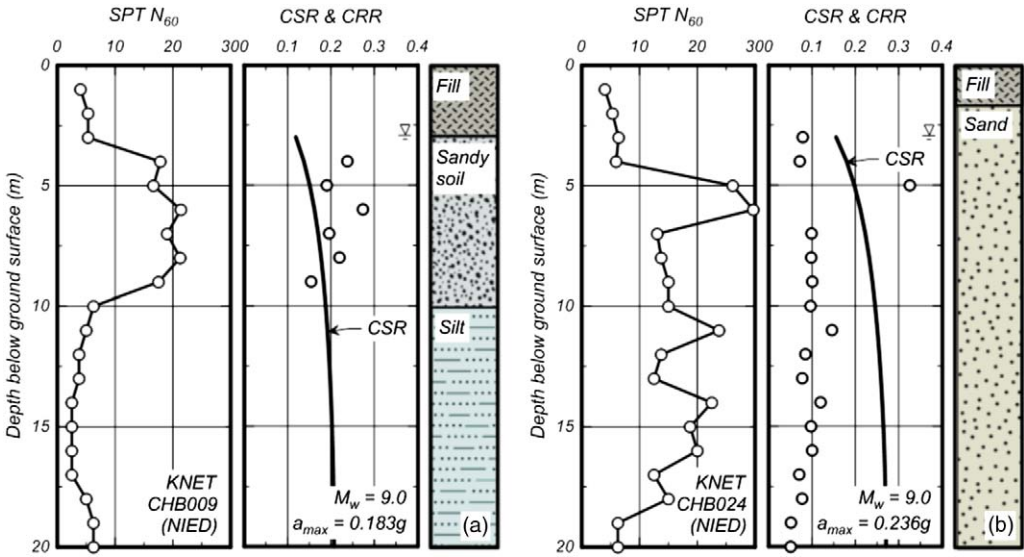


Figure 4. Soil profiles, SPT data, and liquefaction analysis results for: (a) station CHB009, and (b) station CHB024 (soil profiles from KNET, NIED 2011).

analyzed using cyclic softening procedures. For the first scenario, a liquefaction analysis using the procedures from Idriss and Boulanger (2008) indicates that the silt layer would be expected to have liquefied throughout its full depth (factors of safety against liquefaction, FS_{liq} , ranging from 0.3 to 0.45) and the expected surface settlement would have been about 47 cm. For the second scenario, cyclic softening analyses using the procedures from Idriss and Boulanger (2008) indicate that the silt layer would be expected to be safe against cyclic softening (i.e., peak shear strains less than 3%) and would develop relatively small reconsolidation settlements, provided its over-consolidation ratio (OCR) was greater than about 1.2. This second scenario is clearly in better agreement with the absence of observable ground deformations at the site and is considered quite reasonable for this geologic setting.

The liquefaction analysis results shown in Figure 4a are based on this second scenario, such that the potential role of the overlying sandy soil layer can now be examined separately from the underlying silt. The $FS_{liq} = CRR/CSR$ was greater than unity for all but one of the SPT blow counts in the sandy layer, and the expected surface settlement is about 3 cm, with half of this settlement occurring in the bottom 1 m of the sandy stratum. It is possible that liquefaction occurred in this lower portion of the sandy stratum and did not manifest itself at the surface, but it is also possible that the absence of liquefaction evidence can be explained by a refined site characterization (e.g., higher fines content for that sample), an improved understanding of magnitude scaling (duration) factors for silty sands (e.g., at $M_w = 9.0$, the MSF would be 0.67 for sands and 0.95 for clays, such that a refined estimate for silty sands may be important at such large earthquake magnitudes), or an improved estimate of the earthquake-induced CSR based on site response analyses. These results illustrate how the reliable interpretation and analysis of these sites requires additional site characterization

data, including fines content and plasticity information that are not currently available for the different strata.

KNET station CHB024 (Figure 1a and Table 1), just a short distance away from CHB009, is an example of a liquefaction site, as evidenced by the extensive surface ejecta and ground cracking shown in the post-earthquake photograph in Figure 2b. The acceleration time series recorded at the station (NIED 2011), as shown in Figure 3, exhibit a clear change in site response characteristics (e.g., deamplification and period elongation) at about 130 s, which is attributed to the triggering of liquefaction. The PGA at the site was 0.237 g. The soil profile consists of about 1.5 m of fill, overlying a thick sand layer (Figure 4b). The water table is estimated to be at a depth of about 3 m. The SPT blow counts, which are assumed to correspond to a typical energy ratio of 75%, are generally less than 20, as indicated in Figure 4b. Excluding a dense layer between approximately 4–7 m, the CRRs are all lower than the earthquake-induced CSRs computed using the procedures from Idriss and Boulanger (2008). The fines content of the sand is not available, so it was assumed to be 5% based on its visual description. The analysis results are reasonably consistent with the observed field behavior in that the $FS_{liq} = CRR/CSR$ was well below unity for most of the sand stratum. The predicted free-field surface settlement, again using the procedures from Idriss and Boulanger (2008), is about 50 cm, which is greater than generally observed at the site (near adjacent buildings on pile foundations). The overestimation of surface settlements could be attributed to the expectation that liquefaction may initiate in certain depth intervals and not progress throughout the entire stratum due to the reduction in dynamic stresses following liquefaction triggering. Additional information regarding post-liquefaction settlement analyses is provided below. More detailed analysis of site response effects will require additional site characterization data that is not currently available.

These two stations are illustrative of the needs for additional site characterization data at many of the strong ground motion recording stations listed in Tables 1 and 2 in order to develop them into high-quality case histories appropriate for future detailed dynamic analyses. Subsequent field efforts focused on providing improved characterization at a small subset of select ground motion recording stations in Urayasu City are described in the following section.

LIQUEFACTION IN URAYASU CITY

Urayasu City, located in the Tokyo Bay region (Figure 1b), experienced significant and widespread liquefaction damage during the earthquake. Liquefaction damage included ground settlements up to 60 cm, settlement/tilting of wooden and reinforced concrete structures on shallow foundations, and rupture of underground utilities from differential settlements or flotation. The severity and distribution of liquefaction damage was strongly influenced by thickness and consistency of reclaimed soil deposits (i.e., fills), soft soil amplification, and presence of ground improvement measures (Tokimatsu and Katsumata 2012). Ground motions in the city were recorded by 17 SMS; one was a KNET station (CHB008), and 16 were from the private network of the Keiyo Gas Co., Ltd. Thirteen of these sites had surface evidence of liquefaction, while four had no surface evidence of liquefaction or ground failure (Tables 1 and 2). These ground motions, coupled with intense mapping and site

characterization efforts by Japanese and GEER researchers, make Urayasu City a unique and well-documented liquefaction study area.

GEOLOGIC CONDITIONS

The majority of Urayasu City is comprised of reclaimed land. The temporal sequence of fill deposits is illustrated in Figure 5. The city consists of three towns: (1) Moto-Machi constructed on native soils, (2) Naka-Machi constructed on land reclaimed in Phase I between 1964 and 1975, and (3) Shin-Machi constructed on land reclaimed in Phase II between 1976 and 1980 (Tokimatsu et al. 2012, Tokimatsu and Katsumata 2012). Figure 6 shows a cross section through the region oriented diagonally from NW to SE. The fills and some alluvial sands (Fs + As) are generally less than 10 m thick, except in Shin-Machi near Akemi, where the aboveground fill is significantly thicker. Most of fills appear to be comprised of silty sands to sandy silts placed with hydraulic means, as shown by photographs in Ishihara et al. (2011). Fines contents of the surface ejecta after the earthquake generally ranged from 15% to 70% and were nonplastic, meaning the plastic limit was not measurable (Tokimatsu et al. 2012). The fills are underlain by a stratum of soft to firm clay (Ac) ranging from about 10- to 40-m thick, which is in turn underlain by Pleistocene deposits (Ds) with SPT blow counts greater than 50. The depth to Pleistocene materials varies considerably across the city, ranging from about 20 m below the ground surface near the original shoreline in Moto-Machi to approximately 60 m below the ground surface in parts of Naka-Machi and Shin-Machi. The ground water levels are generally within 1–3 m from the ground surface (Tokimatsu et al. 2012).

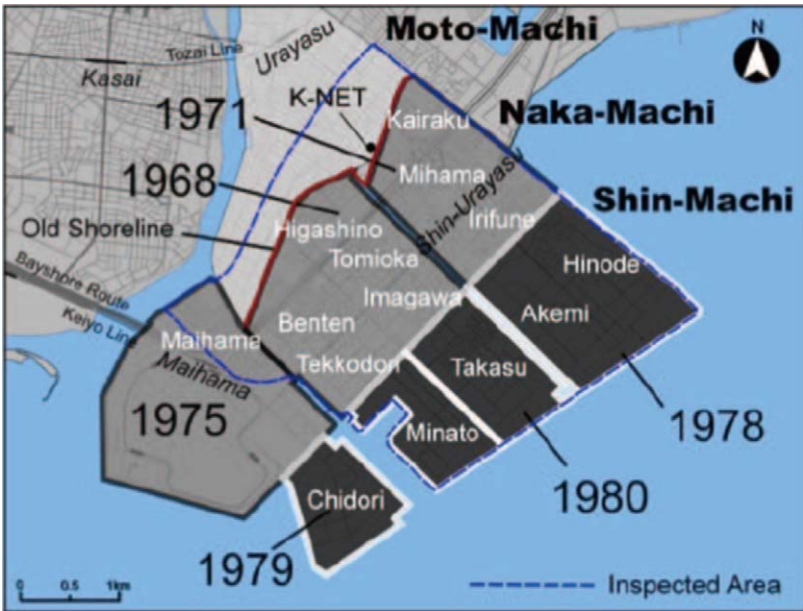


Figure 5. Sequence of fill placement in Urayasu (Tokimatsu and Katsumata 2012).

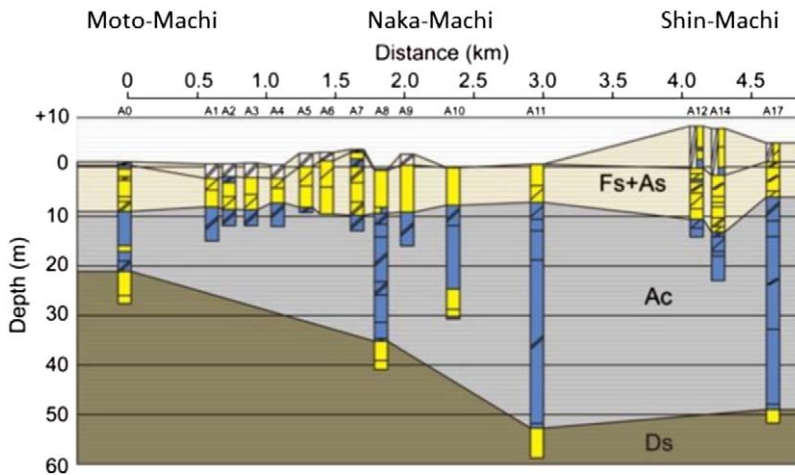


Figure 6. Geologic cross section across Urayasu (after Tokimatsu and Katsumata 2012).

OBSERVED EFFECTS

The city of Urayasu experienced particularly extensive damage to buildings, utilities, and other infrastructure due to liquefaction and has subsequently been the subject of detailed studies by several investigators (e.g., Tokimatsu and Katsumata 2012, Ishihara et al. 2011). A liquefaction severity map detailing areas of extensive, moderate, slight, and no liquefaction is shown in Figure 7. The old shoreline between reclaimed land (i.e., surficial fill soils) and native soils was found to correspond to the boundary of observed liquefaction. Thus, liquefaction of native soils in Moto-Machi was generally not observed, whereas liquefaction in the reclaimed fills ranged from extensive to no liquefaction.

Ground surface settlements relative to buildings supported on pile foundations varied significantly across the city. The photographs in Figure 8 illustrate a particularly interesting case where the ground settled about 30 cm relative to a building on piles (gray building in left photo), while an adjacent three-story building on a mat foundation tilted and settled an additional 40 cm relative to the ground surface (i.e., approximately 70 cm of total settlement). This case clearly illustrates potential problems with the common practice of assuming shallow foundation settlements can be predicted by computing free-field (i.e., volumetric strain) ground surface settlements alone, without including the effects of soil-structure interaction beneath the shallow foundation.

Large numbers of residential buildings exhibited tilts in addition to settlements, as illustrated by the photograph in Figure 9 (left). Tilts of up to 1 to 3 degrees were observed in many cases for residential homes. The structures generally appeared to be free from structural damage, which is attributed to the common foundation design illustrated by the photograph in Figure 9 (right). This foundation was comprised of a 20-cm thick reinforced concrete mat with stiff reinforced concrete perimeter and tie beams. Foundations like these tend to be stiff and strong enough to withstand substantial settlements and tilting while minimizing



Figure 7. Liquefaction severity map of Urayasu City with the locations of strong ground motion stations (liquefaction severity after Tokimatsu and Katsumata 2012).



Figure 8. Differential settlements between a gray building on piles, a brown building on a shallow foundation (brown building on the right), and the ground surface in Urayasu (GEER 2011).



Figure 9. (a) Tilt and settlement of a residential home in Urayasu, and (b) foundation for a residential home in construction (GEER 2011).

distortion of the superstructure. Many of these structures can be re-leveled without the need to rebuild the superstructure.

SPT DATA AND LIQUEFACTION ANALYSES

Tokimatsu et al. (2012) presented liquefaction triggering analyses for many SPT boring logs from across Urayasu City, as shown in Figure 10. The information is organized left to right by districts (refer to Figure 5) generally progressing from Moto-Machi (native soils) to Shin-Machi (fills). The raw SPT blow counts (N -values) are provided in the top plots, while the liquefaction triggering analyses using the mean SPT N -values within each district are provided in the bottom plots. Notice that the triggering analysis for the mean profile in the district of Urayasu Station generally indicates factors of safety greater than 1.0, consistent with observations of no ground failure in the native soil deposits. However, some of the individual SPT profiles in the native soils appear to be susceptible to liquefaction based on penetration resistance and general soil type.

Consider, for example, the soil profile beneath strong motion station KNET CHB008, which is located just inside the old shoreline in the native soil deposits of Moto-Machi (location shown in Figure 7). There was no surficial evidence of ground failure at this SMS, as shown by the post-earthquake photograph in Figure 11a, and the recorded accelerations also contained no evident effects of liquefaction (Figure 11b). The soil profile consists of 1.0 m of fill, overlying 1.25 m of sandy soil, overlying 2.25 m of sand, overlying 3.5 m of sandy soil on top of a thick silt layer (Figure 11c). The water table is estimated to be at a depth of about 2 m. The SPT N_{60} values, based on an assumed typical energy ratio of 75%, were 18–26 in the 2.25-m thick sand layer, about 10 in the underlying 3.5-m thick sandy soil layer, and about 5 or less in the underlying silt layer. To perform a liquefaction evaluation, the fines content of the sand was assumed to be 5% and the fines content of the underlying sandy soil was assumed to be 25%. The plasticity of the silt strata is not available, so two scenarios were considered: (1) the silt is nonplastic such that it should be analyzed using liquefaction correlations, or (2) the silt is sufficiently plastic that it should instead

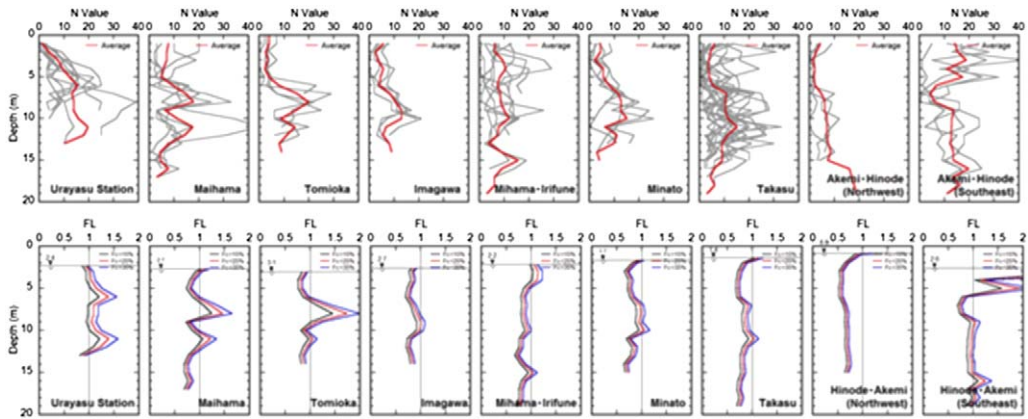


Figure 10. Subsurface profiles of SPT blow count (top) and estimated mean factor of safety against liquefaction (bottom) for various parts of Urayasu City (Tokimatsu et al. 2012).

be analyzed using cyclic softening procedures. For the first scenario, a liquefaction analysis using the procedures from Idriss and Boulanger (2008) indicates that the silt layer would be expected to have liquefied throughout its full depth (factors of safety against liquefaction, FS_{liq} , ranging from 0.33 to 0.49), and the expected surface settlement would have been about 61 cm. For the second scenario, cyclic softening analyses using the procedures from Idriss and Boulanger (2008) indicate that the silt layer would be expected to be safe against cyclic softening (i.e., peak shear strains less than 3%) and would develop relatively small reconsolidation settlements provided its OCR was greater than about 1.2. This second scenario is clearly in better agreement with the absence of observable ground deformations at the site, similar to what was found for the CHB009 site presented in Figure 4. The liquefaction analysis results shown in Figure 11c are based on this second scenario, such that the potential role of the overlying sand and sandy soil layers can now be examined independently of the silt. The CRR and CSR values computed for the sand and sandy soil layers using the procedures from Idriss and Boulanger (2008) are compared in Figure 11c; the $FS_{liq} = CRR/CSR$ values were significantly greater than 1.0 in the sand layer, but only about 0.65–0.80 in the 3.5-m thick sandy soil layer. The predicted surface settlement, using the procedures from Idriss and Boulanger (2008), is about 8 cm. These computed FS_{liq} and settlement values are not consistent with the lack of liquefaction evidence at this SMS, which may simply reflect limitations in the assumptions that were required to perform the analyses. These results again illustrate how the reliable interpretation and analysis of these SMS sites will require additional site characterization data, including fines content and plasticity information for the different strata, an improved understanding of magnitude scaling (duration) factors for silty sands, and improved estimates of the earthquake-induced CSR values.

Katsumata and Tokimatsu (2012) computed expected ground settlements at many locations in Urayasu with SPT data using the simplified procedures outlined in the *Recommendations for Design of Building Foundations* of the Architectural Institute of Japan (AIJ; Tokimatsu and Asaka 1998). They compared these estimates with settlement observations

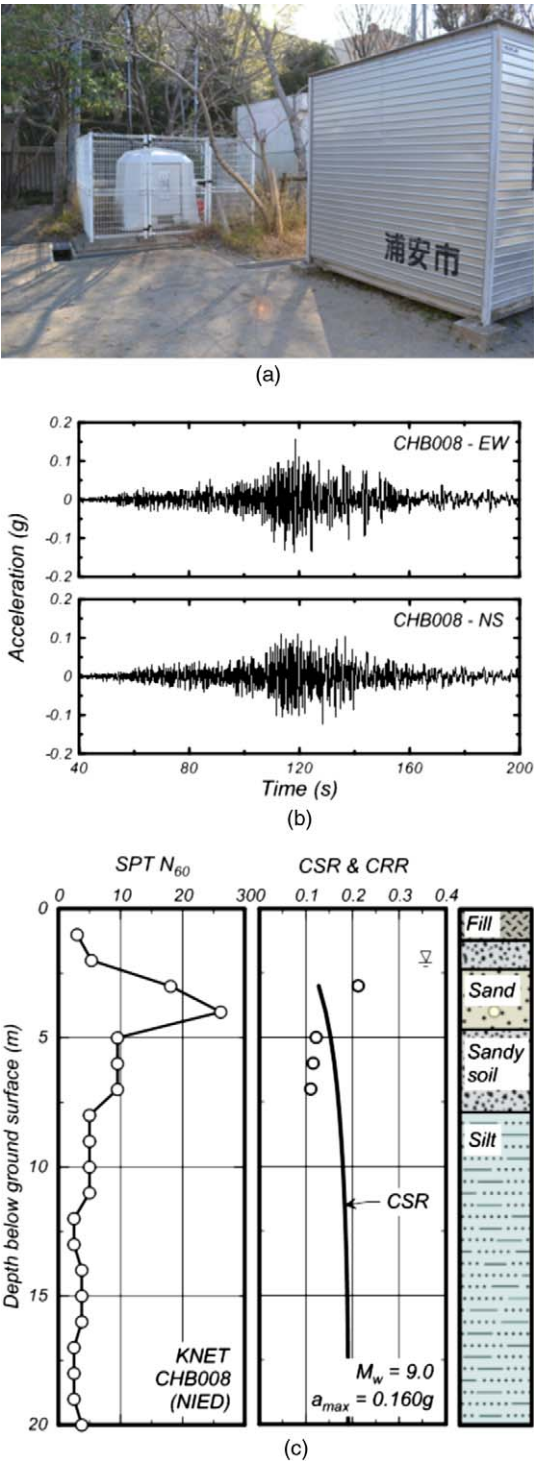


Figure 11. KNET Station CHB008: (a) Photograph showing no surface evidence of liquefaction, (b) horizontal acceleration recordings, and (c) liquefaction analysis of SPT data (motions and profile KNET, [NIED 2011](#)).

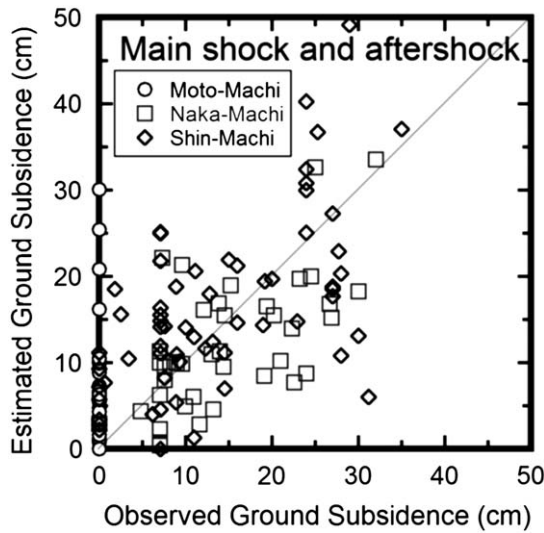


Figure 12. Comparison of observed and estimated ground surface settlements using AIJ procedures and including the effects of the $M_w = 7.7$ aftershock (Katsumata and Tokimatsu 2012).

derived from terrain models made before and after the earthquake using airborne LiDAR surveys. These comparisons are provided in Figure 12. The estimated settlements primarily ranged from 0 cm to about 35 cm, and the observed free field settlements also ranged from about 0 cm to 35 cm. However, the data points are quite dispersive without a strong correlation or bias between estimated and observed settlement. Of particular interest are the many “false-positive” estimates of liquefaction-induced settlements in the native soils of Moto-Machi, where settlements up to 30 cm were estimated from some SPT data while observed settlements were essentially zero (small). These differences between computed and observed settlements warrant further study and may in part reflect local variations in soil consistency, fines plasticity, age, ground shaking intensity, measurement uncertainties, and other factors that are not fully characterized at this time. For individual sites, differences could also result from dispersion in the settlements inferred from the LiDAR data, which have been shown to have standard deviations in the range of 6–20 cm under “best case” conditions involving minimal vegetative cover (Stewart et al. 2009).

Ishihara et al. (2011) similarly analyzed a set of SPT data and reported that SPT-based liquefaction analysis procedures did not appear to explain the differences in liquefaction-induced settlements across the various natural alluvial and fill materials of different ages and fines content in Uraysu. This is consistent with Dobry’s (2012, personal communication) suggestion that loose natural soils in active seismic areas like California and Japan may in fact be more resistant to liquefaction than younger artificial fills of similar stiffness due to the significant effects of pre-shaking on liquefaction resistance. Resolution of differences in liquefaction resistance between native sediments and fill soils may require more detailed site characterization data and possibly more basic research on the effects of aging, pre-shaking and fines content.

SEISMIC VELOCITY TESTING

Surface wave testing was performed by several of the authors at 56 locations in Japan in the fall of 2011, with 28 of those locations in Urayasu City. A combination of active source spectral analysis of surface waves (SASW) testing and multi-channel analysis of surface waves (MASW) testing was used. Details of the data collection and data analysis procedures may be found in [Kayen et al. \(2012b\)](#). The 28 surface wave-derived V_s profiles in Urayasu have been used to investigate differences in the small-strain shear stiffness of natural soils and different aged fills with various liquefaction severity indices.

The surface wave testing locations are shown relative to the different ages of reclaimed/native soils, as well as the various liquefaction severity indices, in Figure 13. Note once again, that ground failure was not observed in the native soil deposits of Moto-Machi north-west of the old shoreline. However, as discussed above, some of these deposits might have been expected to liquefy under the ground motions experienced during the earthquake based on SPT resistance in the absence of soil plasticity information. Therefore, median V_s profiles were calculated from the individual V_s profiles within each phase of fill to investigate if small-strain aging effects, which might not be reflected in SPT blow counts, could possibly explain the differences in performance between the reclaimed land and the native soils.

The median, overburden-corrected shear wave velocity (V_{s1}) profiles for the native Phase I and Phase II soil zones are compared in Figure 14a. The number of profiles used to compute the median V_{s1} values are provided inside parentheses in the legend. The median V_{s1} profiles for all three soil zones are almost identical down to about 12 m. In addition, the V_{s1} profiles are well below the recommended upper-bound corrected shear wave velocity for liquefaction (i.e., $V_{s1}^* = 215$ m/s; [Andrus and Stokoe 2000](#)). These data indicate that significant small-strain aging effects, which might lead to increased liquefaction resistance, cannot be discerned in the median V_{s1} profiles, as all of the soils appear to be loose enough to liquefy down to significant depths based on available V_s -based liquefaction correlations (e.g., [Andrus and Stokoe 2000](#), [Kayen et al. 2012a](#)). Interestingly, the Phase I soils appear on average to be relatively stiffer at depth than the native and Phase II soils (yet still very soft).

The median V_{s1} profiles for the areas with extensive liquefaction and with no ground failure are shown in Figure 14b. While the V_s profiles collected in areas with extensive liquefaction are slightly softer on average near the ground surface, the median V_{s1} profiles for both extensive liquefaction damage and no ground failure are almost identical down to about 12 m depth and are well below $V_{s1}^* = 215$ m/s. These data indicate that significant differences in small-strain shear stiffness do not exist between zones of extensive liquefaction and no liquefaction.

Profiles of V_{s1} obtained from seismic CPT (SCPT) testing at seven SMS, four with evidence of liquefaction and three without evidence of liquefaction or ground failure, are compared in Figure 14c. These data also fail to show a significant difference in shear stiffness between sites with evidence of liquefaction (stations IRF, JAL, TKM, and TKK in Figure 7) and sites without surface evidence of liquefaction or ground failure (stations AKM, HND, and HOS in Figure 7). The one exception is the SCPT V_{s1} profile at station HOS, which is located on native soil deposits well away from the reclaimed land. This V_{s1} profile is significantly stiffer than the others over the top seven meters with velocities greater than $V_{s1}^* = 215$ m/s.

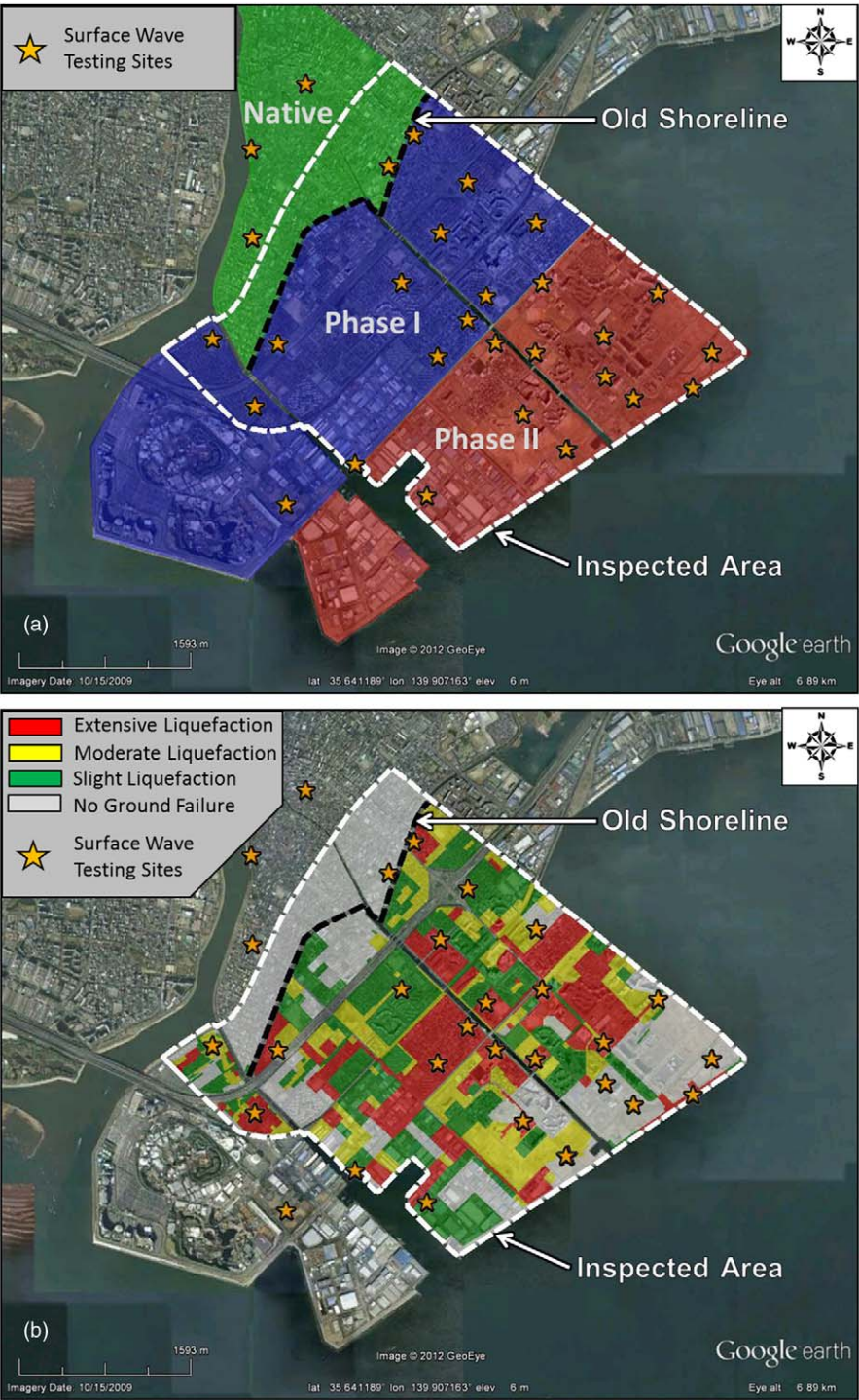


Figure 13. Maps showing surface wave testing locations in Urayasu City relative to: (a) Different ages of reclaimed/native land and (b) severity of liquefaction effects (liquefaction severity after Tokimatsu and Katsumata 2012).

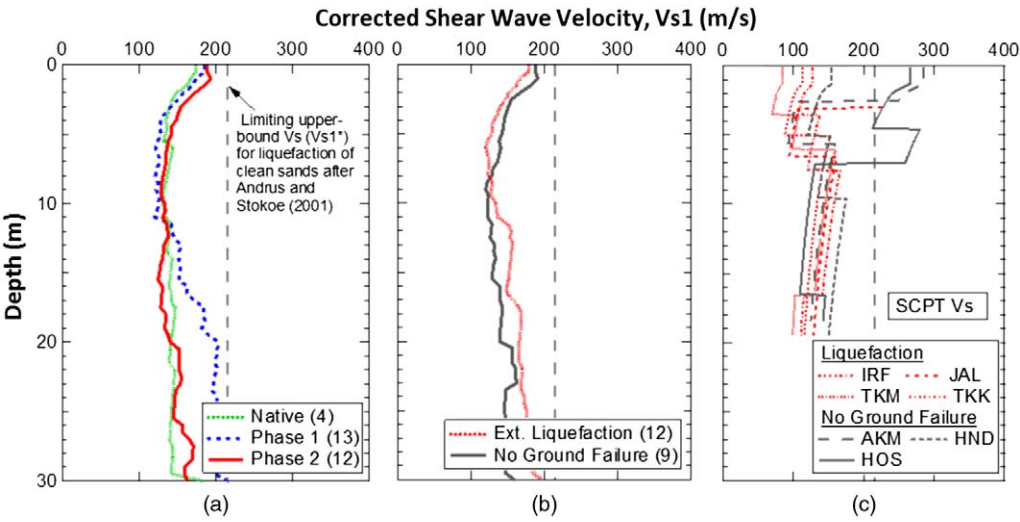


Figure 14. Comparisons of overburden-corrected shear wave velocity (V_{s1}) profiles from Urayasu: (a) Median V_{s1} profiles from surface wave data collected on native soils, phase 1 fills (1964-1975), and phase 2 fills (1976-1980), (b) median V_{s1} profiles from surface wave data collected in locations of extensive liquefaction and locations with no surface evidence of liquefaction or ground failure, and (c) seismic CPT V_{s1} profiles at four SMS that liquefied and three that had no surface evidence of liquefaction or ground failure.

It thus appears that the observed variations in liquefaction effects across Urayasu cannot be differentiated solely on the basis of differences in the soils' small-strain shear modulus. As such, the differences in liquefaction severity, or the lack thereof, are clearly controlled by other factors, such as local variations in ground shaking intensity, soil consistency, fines plasticity, age, foundation types/loads, and other factors that are not yet fully understood. While information on the variation of ground shaking across the city is well constrained (note that the PGAs recorded in Urayasu varied from 0.15 g to 0.27 g at stations that liquefied and from 0.16 g to 0.18 g at stations that did not have surface evidence of liquefaction or ground failure), additional soil information is needed to fully utilize the V_s profiles, refine V_s -based liquefaction triggering analyses on a site-by-site basis, and develop each site into a quality case history.

CPT DATA AND LIQUEFACTION ANALYSES

CPT profiles were obtained at seven SMS locations in Urayasu to more fully investigate some of the factors influencing the observed variations in liquefaction effects; these seven SMS included four with evidence of liquefaction (IRF, JAL, TKM, and TKK in Figure 7) and three without observed ground failure (AKM, HND, and HOS in Figure 7). Profiles for stations HND and HOS (without ground failure) and TKK and TKM (with liquefaction) are shown in Figure 15a-d, respectively, to illustrate the range of soil conditions obtained. Each figure shows the tip resistance (q_t ; corrected for pore pressures behind the tip), sleeve friction ratio (R_f), soil behavior types (SBT) based on Robertson (1990), and the CSR and

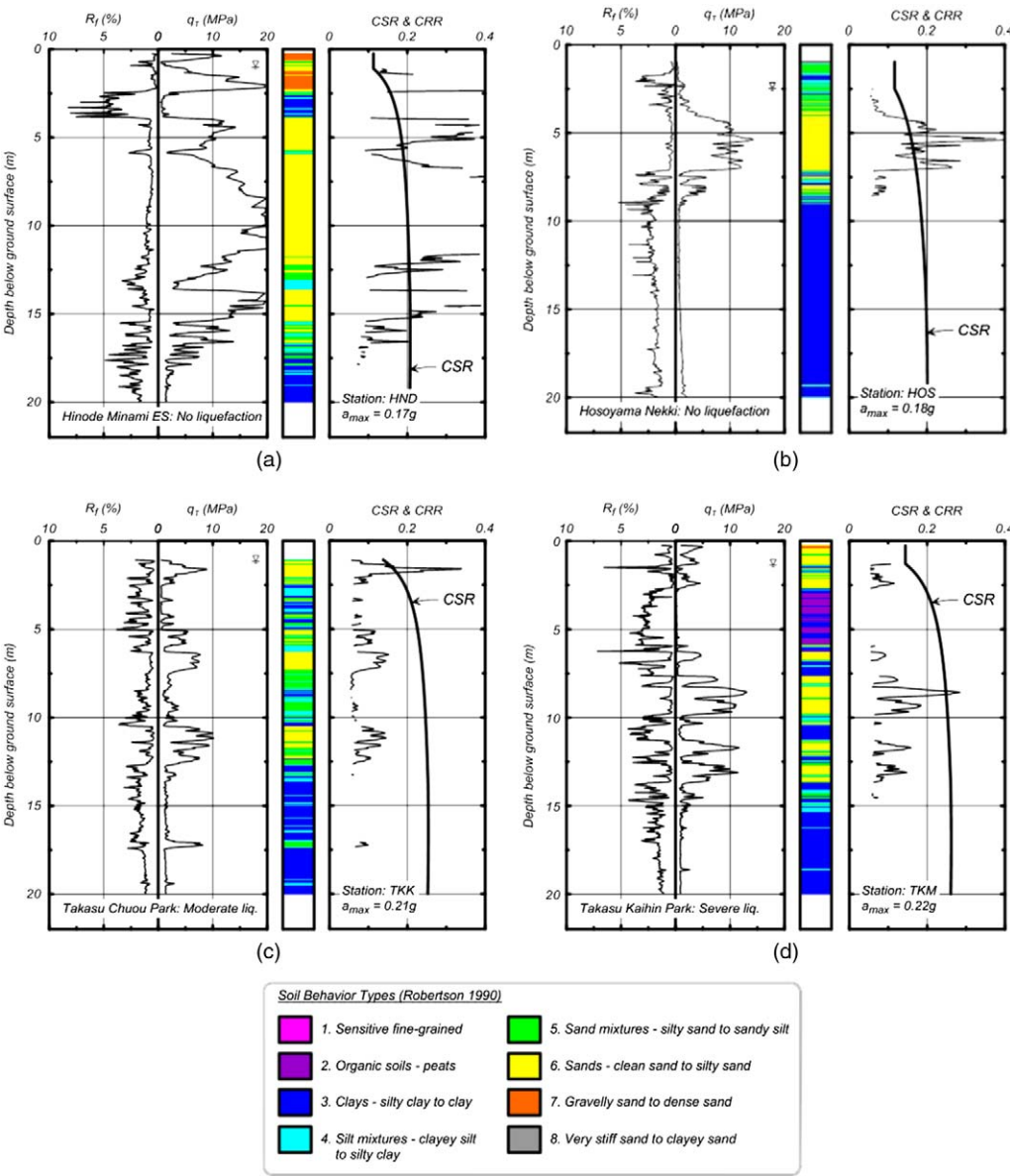


Figure 15. Cone penetration test profiles and liquefaction analyses at four strong ground motion recording stations in Urayasu with (a) no surface evidence of liquefaction or ground failure, (b) no surface evidence of liquefaction or ground failure, (c) moderate liquefaction, and (d) severe liquefaction.

CRR values obtained using the procedures by [Idriss and Boulanger \(2008\)](#). Liquefaction analyses using the procedures by [Robertson and Wride \(1998\)](#) produced slightly greater CRR values but led to the same general observations as discussed below. The liquefaction

analysis results shown in these figures are for the case where the CPT data are analyzed on a point-by-point basis, after which the effects of interfaces and interlayers can be discussed.

The CPT liquefaction analyses for the HND (Figure 15a) and HOS (Figure 15b) stations are generally consistent with the observed absence of ground failure, although they both illustrate some of the common difficulties in analyzing CPT data near interfaces and interlayers. Clay soil types, corresponding to soil behavior type indices (I_c) greater than about 2.6, were identified at depths of 2.5–3.9 m ($I_c \approx 2.9$), 13.1–13.6 m ($I_c \approx 2.6$) and below 17.5 m ($I_c \approx 3.1$) at the HND station and at depths of 1.0–2.4 m ($I_c \approx 2.8$) below 8.6 m ($I_c \approx 3.3$) at the HOS station. For the sand layers, fines contents were estimated by correlation to the I_c value (Idriss and Boulanger 2008) with an Urayasu-specific adjustment upward from the general correlation to give $FC \approx 20\%$, on average. The sand layers at both stations are sufficiently dense that liquefaction triggering would not be expected (i.e., $CRR > CSR$) at points more than about 30 cm from an interface with a clay soil type. The liquefaction analyses for both stations do, however, show that the computed CRR values are less than the CSR values near clay interlayers (e.g., 5.9 m at HND) and in intervals that appear to have finely interlayered sands and clays (e.g., 15.5–17.5 m at HND and 7.2–8.6 m at HOS). The low CRR values in these intervals can represent artifacts that stem from the known limitations in CPT data near such interfaces. The potential settlements due to one-dimensional reconsolidation were computed to be 8 cm and 11 cm at HND and HOS, respectively, based on these point-by-point analysis results. The amount of liquefaction triggering and computed settlements can be reduced to the range of a couple of centimeters if the effects of the clay-sand interfaces are accounted for, such that the computed and observed responses are reasonably consistent when these types of details are appropriately considered.

The CPT liquefaction analyses for the TKK (Figure 15c) and TKM (Figure 15d) stations are also generally consistent with the observations of moderate to severe liquefaction effects. Clay soil types are encountered in numerous layers at these stations, with I_c values being similar to those for the clay soil types at similar depths at stations HND and HOS. Sand layers at the TKK and TKM stations have generally smaller overburden-corrected tip penetration resistances, such that they give generally smaller CRR values than obtained at the HND and HOS stations. The CSR values are also greater at the TKK and TKM stations because the measured peak ground surface accelerations (0.21 g and 0.22 g) are greater than measured at the HND and HOS stations (0.17 g and 0.18 g). The combined effect is that liquefaction would have been expected at the TKK and TKM stations for the observed shaking levels, although these analysis results also have the previously discussed problem of likely overpredicting the extent of liquefaction near clay-sand interfaces. The potential settlements due to one-dimensional reconsolidation were computed to be 29 cm and 20 cm at TKK and TKM, respectively, based on the point-by-point analyses. These values can similarly be reduced significantly by accounting for interface effects, but the remaining settlements would still be consistent with the observation of surface effects.

More detailed examination of the compiled CPT data, in conjunction with analyses of the available SPT and V_s data, are expected to progress as additional site characterization information becomes available. In this regard, it is hoped that the archiving of these CPT and V_s data at the GEER website (<http://geerassociation.org/>) will constitute a valuable resource for future researcher efforts.

SUMMARY

The 2011 $M_w = 9.0$ Tohoku-oki earthquake has generated a large number of high-quality soil liquefaction case histories, including a unique set of ground motion records obtained from seismic stations on geologically recent sediments or fills potentially susceptible to liquefaction. We have presented a list of 21 strong motion stations (SMS) where surface evidence of liquefaction was observed following the earthquake and 17 SMS underlain by geologically recent sediments or fills with shallow ground water where surface evidence of liquefaction was not observed. These ground motion recordings represent a unique set of data that captures the dynamic response and liquefaction of soils during long-duration shaking produced by this $M_w = 9.0$ earthquake. Preliminary liquefaction analyses using existing SPT data available at a few of these stations were presented. The results of these analyses indicate that additional site characterization data (particularly soil plasticity and fines content) are required for many of the SMS before the full value of these ground motion recordings can be realized. We encourage additional data-gathering efforts at these stations so that the engineering community at large can benefit from this valuable data set of ground motions.

We performed seismic cone penetration tests (SCPT) at a subset of seven SMS sites (three SMS sites with no surface evidence of liquefaction and four SMS sites with moderate to severe liquefaction effects) and V_s profiling using surface wave methods at 28 additional locations throughout Urayasu City to supplement pre-existing geotechnical data. The CPT and surface wave testing data will be archived at the GEER website (<http://geerassociation.org/>) for future, more in-depth analyses by interested researchers. Median V_s profiles showed no significant differences in small-strain shear modulus between soils of different ages or between areas of different liquefaction severity. However, once again, additional soil type/plasticity information is still needed to fully understand and utilize the V_s data. The results of preliminary liquefaction analyses using the CPT data at select SMS sites are reasonably consistent with the observed behaviors at these sites. The differences in liquefaction severity across these SMS and across Urayasu native and fill soils are generally attributed to local variations in the intensity of ground shaking, soil consistency, fines plasticity, stress history/pre-shaking, and possibly differences in aging. It is hoped that the compiled and archived data will provide a lasting resource for further research toward fully understanding and interpreting the observed responses at these SMS and their surrounding areas.

ACKNOWLEDGEMENTS

The National Science Foundation (NSF) provided support for geotechnical reconnaissance of this earthquake through a RAPID award to Ross W. Boulanger, UC Davis, and Nick Sitar, UC Berkeley, under grant #CMMI-1138203. NSF supported the field surface wave and CPT testing through a RAPID award to Brady Cox at University of Arkansas, under grant #CMMI-1138168. GEER is supported by the NSF under grant #CMMI-00323914. Any opinions, findings, and conclusions or recommendations expressed in this material are those of the authors and do not necessarily reflect the views of the NSF. Additional support for travel was provided by Fugro, Geosyntec, Kleinfelder, and the U.S. Geological Survey. GEER team members included, in addition to the authors, Pedro Arduino, Dominic Assimaki, Jonathan Bray, Shideh Dashti, Craig Davis, David

Frost, Les Harder, Jr., Youssef Hashash, Laurie Johnson, Keith Kelson, Steven Kramer, Jorge Meneses, Thomas O'Rourke, Ellen Rathje, Kyle Rollins, Isabelle Ryder, Ashley Streig, Joe Wartman, and Josh Zupan. Teams from GEER collaborated with colleagues in Japan and teams from the Earthquake Engineering Research Institute, the Pacific Earthquake Engineering Research Center, the American Society of Civil Engineers, and the Federal Highways Administration.

The Japan Science and Technology Agency provided matching support for collaborative U.S.–Japanese geotechnical reconnaissance through a J-RAPID award to Kohji Tokimatsu. Many individuals and organizations from Japan contributed information and support to this research, including Masanori Hamada, Eiji Kohama, Kazuhiko Kawashima, Kazuo Konagai, Tetsuro Kuwabara, Takashi Nagao, Shingo Satou, Toshiro Suzuki, Yasuo Tanaka, Hajime Tanaka, Takahiro Sugano, Ikuo Towhata, Akihiro Takahashi, Jiro Takemura, Keiichi Tamura, Hideo Tokuyama, Toru Tomoika, Kiyoshi Yamada, Yoshimichi Tsukamoto, Mitsutoshi Yoshimine, and M. Yoshizawa, as well as numerous graduate students. Keiyo Gas Co., Ltd., generously provided information on strong ground motion recordings from their private network, and the City of Urayasu provided assistance and information, as well as permission, for our site investigations. The above assistance and support is greatly appreciated.

REFERENCES

- Andrus, R. D., and Stokoe, K. H., II, 2000. Liquefaction resistance of soils from shear wave velocity, *Journal of Geotechnical and Geoenvironmental Engineering*, ASCE, **126**, 1015–1025.
- Boulanger, R., 2012. Liquefaction in the 2011 Great East Japan Earthquake: Lessons learned for U.S. practice, *Proc., Intl. Symposium on Engineering Lessons Learned from the 2011 Great East Japan Earthquake*, 1–4 March 2012, Tokyo, Japan, 601–606.
- Dobry, R., 2012. Personal communication.
- Geotechnical Extreme Events Reconnaissance (GEER) Association, 2011a. *Quick Report 1: Geotechnical Quick Report on the Kanto Plain Region during the March 11, 2011, Off Pacific Coast of Tohoku Earthquake, Japan*, Report GEER-025a, <http://geerassociation.org/>.
- Geotechnical Extreme Events Reconnaissance (GEER) Association, 2011b. *Quick Report 2: Preliminary Observations of Levee Performance and Damage Following the March 11, 2011 Tohoku Offshore Earthquake, Japan*, Report GEER-025b, <http://geerassociation.org/>.
- Geotechnical Extreme Events Reconnaissance (GEER) Association, 2011c. *Google Earth File (May 10, 2011) for Tohoku Earthquake, Japan*, Report GEER-025b, <http://geerassociation.org/>.
- Geotechnical Extreme Events Reconnaissance (GEER) Association, 2011d. *Geotechnical Effects of the Mw 9.0 Tohoku, Japan, Earthquake of March 11, 2011*, EERI Special Earthquake Report, Earthquake Engineering Research Institute, September, 12 pp.
- Idriss, I. M., and Boulanger, R. W., 2008. *Soil Liquefaction during Earthquakes*, MNO-12, Earthquake Engineering Research Institute, Oakland, CA.
- Ishihara, K., Araki, K., and Bradley, B., 2011. Characteristics of liquefaction-induced damage in the 2011 Great East Japan Earthquake, *Geotec Hanoi*, October, ISBN 978-604-82-000-8.
- Katsumata, K., and Tokimatsu, K., 2012. Relationship between seismic characteristics and soil liquefaction of Urayasu City induced by the 2011 Great East Japan Earthquake, *Proc., 9th International Conference on Urban Earthquake Engineering/4th Asia Conference on Earthquake Engineering*, 6–8 March 2012, Tokyo, Japan, 601–606.

- Kayen, R., Moss, R. E. S., Thompson, E. M., Seed, R. B., Cetin, K. O., Der Kiureghian, A., Tanaka, Y., and Tokimatsu, K., 2012a. Shear wave velocity-based probabilistic and deterministic assessment of seismic soil liquefaction potential, *Journal of Geotechnical and Geoenvironmental Engineering*, ASCE, in press.
- Kayen, R. E., Ishihara, K., Stewart, J. P., Tokimatsu, K., Cox, B. R., Tanaka, Y., Kokusho, T., Mason, H. B., Moss, R. E. S., Zekkos, D., Wood, C. M., Katsumata, K., Estevez, I. A., Cullenward, S. S., Tanaka, H., Harder, L. F., Kelson, K. I., and Kishida, T., 2012b. Geotechnical deformations at ground failure sites from the March 11, 2011 Great Tohoku Earthquake, Japan: Field mapping, LiDAR modeling, and surface wave investigation, *Proc., 9th International Conference on Urban Earthquake Engineering/4th Asia Conference on Earthquake Engineering*, 6–8 March 2012, Tokyo, Japan.
- National Research Institute for Earth Science and Disaster Prevention (NIED), 2011. <http://www.bosai.go.jp>, Japan.
- Robertson, P. K., 1990. Soil classification using the cone penetration test, *Canadian Geotechnical Journal* **27**, 151–58.
- Robertson, P. K., and Wride, C. E., 1998. Evaluating cyclic liquefaction potential using the cone penetration test, *Canadian Geotechnical Journal* **35**, 442–459.
- Stewart, J. P., Hu, J., Kayen, R. E., Lembo, Jr., A. J., Collins, B. D., Davis, C. A., and O'Rourke, T. D., 2009. Use of airborne and terrestrial LIDAR to detect ground displacement hazards to water systems, *J. Surveying Engineering*, ASCE, **135**, 113–124.
- Stewart, J. P., Midorikawa, S., Graves, R. W., Khodaverdi, K., Kishida, T., Miura, H., Bozorgnia, Y., and Campbell, K. W., 2013. Implications of M_w 9.0 Tohoku-oki, Japan, earthquake for ground motion scaling with source, path, and site parameters, *Earthquake Spectra*, **29**, S1–S21.
- Tokimatsu, K., and Katsumata, K., 2012. Liquefaction-induced damage to buildings in Urayasu City during the 2011 Tohoku Pacific Earthquake, *Proc., Intl. Symposium on Engineering Lessons Learned from the 2011 Great East Japan Earthquake*, 1–4 March 2012, Tokyo, Japan, 665–674.
- Tokimatsu, K., Tamura, S., Suzuki, H., and Katsumata, K., 2012. Geotechnical problems in the 2011 Tohoku Pacific earthquake, *Proc., 9th International Conference on Urban Earthquake Engineering/4th Asia Conference on Earthquake Engineering*, 6–8 March 2012, Tokyo, Japan, 49–61.
- Tokimatsu, K., Tamura, S., Suzuki, H., and Katsumata, K., 2011. *Quick Report on Geotechnical Problems in the 2011 Tohoku Pacific Ocean Earthquake*, Research Reports on Earthquake Engineering, CUEE, Tokyo Institute of Technology, No. 118, 21–47 (in Japanese).
- Tokimatsu, K., and Asaka, Y., 1998. Effects of liquefaction-induced ground displacements on pile performance in the 1995 Hyogoken-Nambu earthquake, *Soils and Foundations* **38**, Special Issue, 163–177.
- Tsukamoto, Y., Kawabe, S., Kokusho, T., and Araki, K., 2012. Observed performance and estimated soil properties of reclaimed and natural deposits at Kamisu City during 2011 Great East Japan Earthquake, *Proc., Intl. Symposium on Engineering Lessons Learned from the 2011 Great East Japan Earthquake*, 1–4 March 2012, Tokyo, Japan, 143–146.

(Received 30 April 2012; accepted 17 October 2012)